minerals

MDPI

*Supplementary Materials*

# Gas Barrier Properties of Multilayer Polymer–Clay Nanocomposite Films: A Multiscale Simulation Approach

**Andrey Knizhnik[1,2], Pavel Komarov[3,4,*], Boris Potapkin[1,2], Denis Shirabaykin[1], Alexander Sinitsa[1,2] and Sergey Trepalin[1,5]**

[1]Kintech Lab Ltd, Moscow, 123298 Moscow, Russia
[2]National Research Center "Kurchatov Institute", 123182 Moscow, Russia
[3]Institute of Organoelement Compounds RAS, 119991 Moscow, Russia
[4]General Physics Department, Tver State University, Sadovy str. 35, 170002 Tver, Russia
[5]All Russian Institute for Scientific and Technical Information RAS, 125215, Moscow, Russia
[*]Correspondence: pv_komarov@mail.ru

Here is additional information about our study.

## S1. Mechanism of Gas Penetration in Hybrid Organic-Inorganic Multilayer Thin Films

Figure S1 shows the mechanism of gas permeation in hybrid organic-inorganic multilayer thin films [27, 52]. Although an ideal layer of an inorganic material (Figure S1b) is nearly impermeable to molecules, it can contain defects such as holes and cracks. The lower the number of defects in the inorganic layers, the lower the permeability of the hybrid barrier layer. In this case, due to the appearance of nonuniform concentrations of molecules near holes (due to interaction with the defect), the flux through holes $\Gamma_{hole}$ can be greater than the flux determined by their geometric characteristics:

$$\Gamma_{hole}(\theta_{hole}, R_{hole}) = \theta_{hole} \cdot S(R_{hole}) \cdot \Gamma_0, \quad \text{(S1)}$$

where $\theta_{hole}$ is the surface fraction of holes in the inorganic layer, $R_{hole}$ is the hole radius, $\Gamma_0$ is the flux in the absence of an inorganic layer, $S(R_{hole}) > 1$ is the hole capture factor, which is equal to the ratio of the effective area of the hole to the real one.

Experimental results show that the use of coatings with several inorganic layers makes it possible to reduce the permeability of the coating, as shown in Ref. [53] for $Al_2O_3$/polymer bilayers.

Furthermore, according to experimental studies [34], the permeability of coatings with inorganic layers depends on their bending, which may be related to the appearance of new defects, such as cracks, due to large deformation forces (see Figure S2a). To minimize this effect, it has been proposed to optimize the coating structure so that the inorganic layer is closer to the zero stress level (neutral level) in the film, as shown in Figure S2b.

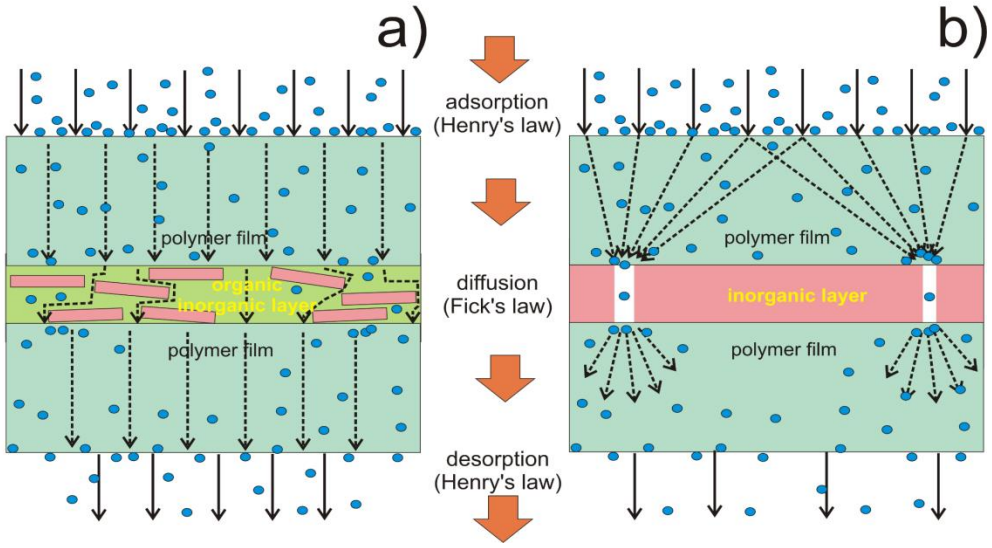


**Figure S1.** The mechanism of gas permeation in hybrid multilayer thin films containing: (**a**) an organic-inorganic layer (polymer filled with clay particles, shown as brown bricks); and (**b**) an inorganic layer with defects (the effect of nonuniform concentrations of molecules near holes is shown schematically). Permeation consists of three steps: (1) adsorption of the gas (blue spheres) on the surface of the barrier material, (2) diffusion of the sorbed gas molecules (dotted arrows), and (3) desorption from the opposite surface of the barrier material.

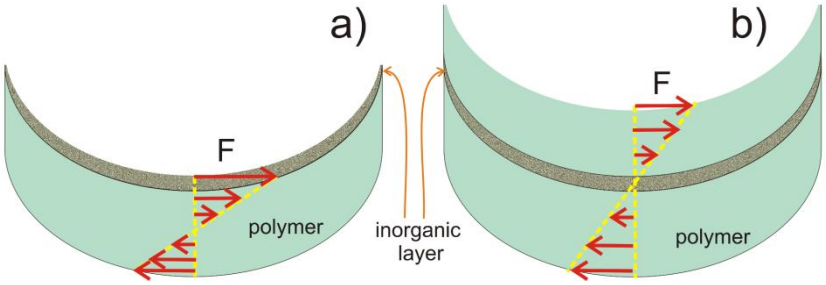


**Figure S2.** Variation of stress F in the inorganic layer depending on its position in the film: (**a**) on the surface, and (**b**) in the central part.

## S2. Gas Permeability Mechanism of Thin Polymer Films

The rate of gas permeation through the polymer layer is determined by the permeability coefficient $P$ (permeability), which is the product of the diffusion parameters $D$ and the solubility $S$ of the gas in the material.

The sorption or solubility coefficient $S$ indicates how much gas molecules can be absorbed by the material. It is defined as the concentration $C$ of the sorbed gas per unit volume of the material in equilibrium with gas molecules of a given pressure $p$ or fugacity $f$:

$$S = C/f \cong C/p, \tag{S2}$$

where the ideal-gas approximation works for sufficiently small $p$. Thus, in most practical applications, it is often assumed that it is acceptable to replace $f$ by $p$.

The solubility coefficient $S$ can be independent of $C$ (Henry's law):

$$S = k \cdot p. \tag{S3}$$

where $k$ is Henry's constant. This can be considered an "ideal case": in contrast to the case of solubility in the polymer material considered here, the concentration of a solute generally has a more complex relationship with the external pressure of the gas, but, for historical reasons, the solubility coefficient is often referred to as Henry's constant.

The diffusion coefficient $D$ is a measure of the mobility of the penetrant molecules in the polymer layer. From a macroscopic thermodynamic point of view, it is assumed that the sorbed gas molecules move at speed $U_x$ under the action of a driving force $\partial\mu/\partial x$ (the gradient of the chemical potential of the penetrant in the material) against the resistance of the polymer matrix, which is measured as the "friction coefficient" $F$. Thus, for a position $x$ inside the layer ($0 < x < l$, where $l$ is the thickness of the layer), the flux density (i.e. the amount of gas transferred through a unit cross-sectional area per unit time) is given by the diffusion coefficient $D$:

$$J_x = -D\cdot\partial C/\partial x\cdot U_x C = -C/F\cdot\partial\mu/\partial x = -D_T C/f\cdot\partial f/\partial x = -D_T S\cdot\partial f/\partial x \cong -P\,\partial p/\partial x, \quad \text{(S4)}$$

where:

$$\mu = \mu^{(g)} = \mu^{0(g)} + RT\ln f \approx \mu^{0(g)} + RT\ln p. \quad \text{(S5)}$$

The "thermodynamic" diffusion coefficient $D_T$ is introduced as $D_T = RT/F$ ($R$ is the gas constant, $T$ is the temperature). Unlike the "classical" phenomenological diffusion coefficient, thermodynamic diffusion coefficients are based on the chemical potential gradient as the driving force. The coefficient of permeability is introduced using the following equation

$$P = D_T S. \quad \text{(S6)}$$

The expression for Fick's first law can be used to establish the relationship between the thermodynamic diffusion coefficient and the phenomenological coefficient $D$:

$$J_x = -D\,\partial C/\partial x = -D_T S\,\partial f/\partial x. \quad \text{(S7)}$$

Then the relationship between $D$ and $D_T$ is:

$$D = D_T S\,df/dC \cong P\,df/dC \cong P\,dp/dC. \quad \text{(S8)}$$

Thus, $D = D_T$, given that

$$S\,df/dC = 1. \quad \text{(S9)}$$

This is true only if $S = const$. It also follows that $D = const$ only if $S = const$ and $D_T = const$ (and hence $P = const$). Such a system is usually called ideal because there is no interaction of the penetrant molecules with each other and because the interaction of the penetrant material is constant (does not depend on the concentration of the penetrant).

In non-ideal diffusion systems, the permeability $P$ (or $D$) varies significantly with the concentration $C$ (or, in some cases, $P$). For such systems, in the general case, $D \neq D_T$ (the degree of discrepancy depends on the magnitude of the deviation from ideal sorption), i.e., strictly speaking, the diffusion coefficient $D$ cannot be considered as the true mobility of the penetrant molecule, although this is often neglected in practice. In this case, the parameter $D$ is usually determined experimentally.

On the basis of these basic rules, it is possible to formulate the problem of predicting the barrier properties of polymeric materials. To determine the permeability of some polymeric material, it is necessary to calculate its diffusion capacity (diffusion coefficient $D$) and ability to dissolve in it (solubility coefficient $S$) for a given penetrant molecule.

**S3. QSPR models**

Table S1 shows the values for the contributions of atoms and groups of atoms to the activation energy, $\Delta E$, see Eqs. (8) – (9), in the Askadskii model [48].

**Table S1.** Contributions of atoms and groups to the activation energy in the Askadskii model.

| Atom or group | Energy (J/mol) |
|---|---|
| H | –90.75 |
| C | 105.85 |
| N | 73.8 |
| O | –20.3 |
| F | –148.8 |
| Si | –388.5 |
| S | –1538 |
| Cl | 109.2 |
| NHCO | –953.7 |
| Double-bond | –452.6 |
| Hydrogen bond | –70.1 |
| Aliphatic cycle | –580.6 |
| Dipole-dipole interaction | –271.9 |
| Backbone aromatic cycle | –502.6 |
| Pendant aromatic cycle | –808.0 |

Figure S3 shows an example of the division of the structural monomer polyethylene terephthalate into fragments and the values of the main parameters necessary to calculate the permeability of water and oxygen using the Bicerano [47] and Askadskii [48] models.

a)

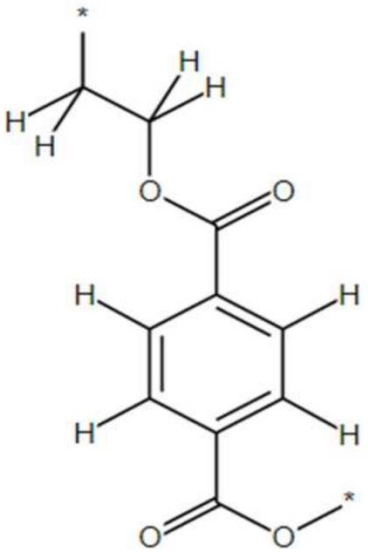

b)

Water permeability, calculated with the Askadsky model

| Atom or fragment | Number of fragments | Energy |
|---|---|---|
| H | 8 | -726 |
| C | 10 | 1058.5 |
| N | 0 | 0 |
| O | 4 | -81.3 |
| F | 0 | 0 |
| Si | 0 | 0 |
| S | 0 | 0 |
| Cl | 0 | 0 |
| Hydrogen bond(NHCO) | 0 | 0 |
| Double bond | 0 | 0 |
| Hydrogen bond (OH) | 0 | 0 |
| Aliphatic cycle | 0 | 0 |
| Dipole-dipole interaction | 2 | -543.8 |
| Aromatic ring in backbone | 1 | -502.6 |
| Aromatic ring in pendant group | 0 | 0 |

Oxygen permeability, Bicerano model

| Atom or fragment | Number of fragments | Energy |
|---|---|---|
| ECoh1 | | 74087 |
| V | | 145.91 |
| Vdw | | 95.04 |
| Nrot | 7 | |
| N | 14 | |
| NC=C | 0 | |
| NbbEster | 2 | |
| X4' | 0 | |
| Nhheqσ | 0 | |
| Ncyanideeqσ | 0 | |
| Nhb,ar | 0 | |
| Nper | | -28 |
| v | | 375.877 |

**Figure S3.** (**a**) Structural formula of polyethylene terephthalate, (**b**) Fragments, specific parameters, and their contributions to the activation energy according to the Askandskii and Bicerano models.

**S4. Screening of Virtually Created Polymers**

One of the most important tasks in the development of new protective coatings is the selection of suitable polymer materials. In our case, to build a multilayer coating model, it is necessary to select polymers with low water vapor and oxygen permeability. This can be done by screening polymer databases using permeability values for these molecules as screening descriptors. However, this is difficult because they do not contain experimental data on the permeability for both water and oxygen. A good solution is to use the quantitative structure-property correlation (QSPR) method to evaluate the properties of the polymers they contain. Unfortunately, this is also difficult, because access to the contents of such databases is often very limited.

As a compromise solution for implementing permeability coefficient screening, we considered the possibility of creating databases of virtually generated polymer monomer units from a set of fragments. To create it, we used polymers that had been used to train the Bicerano model [47] and our algorithm to split monomers into separate fragments described in the next Section S4.1.

In this way, we created a database of virtually constructed polymers. This database is used to calculate the permeability coefficients for oxygen via the Bicerano model and for water via the Askadskii model. The technical details of the work carried out and the results obtained are presented below.

*S4.1. Principles of Generating Polymer Monomer Units*

To screen polymers for oxygen and water vapor permeability, we generate polymer structures using our in-house developed program GENSTRUC. It generates polymer structures based on a database of predefined fragments (see Figure S4) in which hydrogen atoms R1-R8 are replaced by various substituents. All possible combinations of the H, F, and Cl atoms are used as substituents. The program implements two algorithms for generating polymers: (1) random selection of groups and substituents (Monte Carlo), and (2) use of all possible combinations of options for given fragments of the main chain, their number, and substituents. It should be noted that this program is universal and can generate polymer structures of different classes.

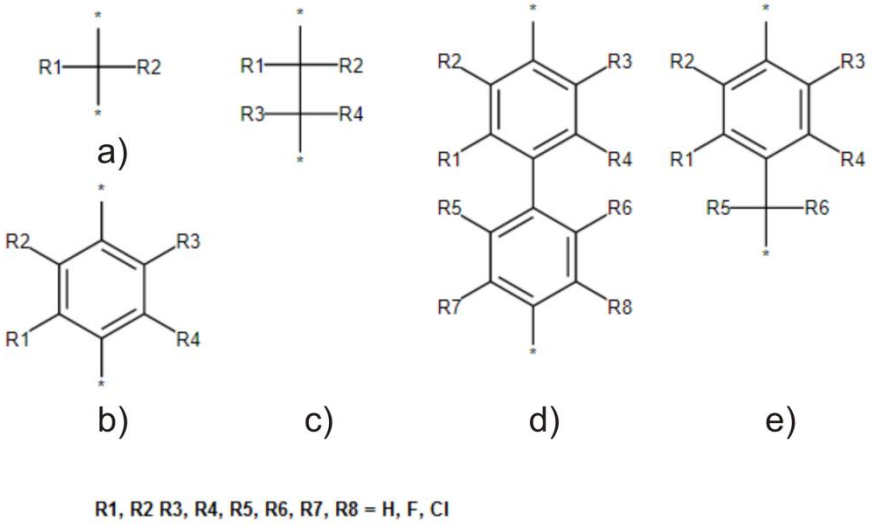


**Figure S4**. Structures of repeating units used for the construction of various polymer monomers: (**a**) polymethylene, (b) poly(para-phenylene) and examples of the backbones of polymers generated by the GENSTRUC program, namely (**c**) polyethylene, (**d**) poly(para,para')diphenylene, and (**e**) poly(paramethylenephenylene). The * symbols indicate the continuation of the chain.

As mentioned above, GENSTRUC uses the database of structural fragments of the backbone and substituents (846 in total) obtained based on the list used to parameterize the Bicerano model, see [47]. For this purpose, all monomers of these polymers were divided into cyclic and acyclic fragments. If there were no cyclic ones, the fragments obtained by all possible combinations (that could reproduce the original repeating unit of the polymer) were taken into account. At the same time, we paid special attention to the analysis of the uniqueness of the considered chemical structures. Let us take a closer look at this problem.

Currently, an approach based on the calculation of the InChIkey identifier [62] is used to determine whether a chemical structure is unique. However, when the experimental InChIkey is used, in the case of some polymers, different ways of representing their structure give the same InChIkey. This example is demonstrated

in Figure S5a for polyethylene glycol. These chemical structures are completely different comonomers. In the general case, when such fragments are combined with others, we obtain polymers with different chemical structures (Figure S5b), which is not acceptable for our purpose.

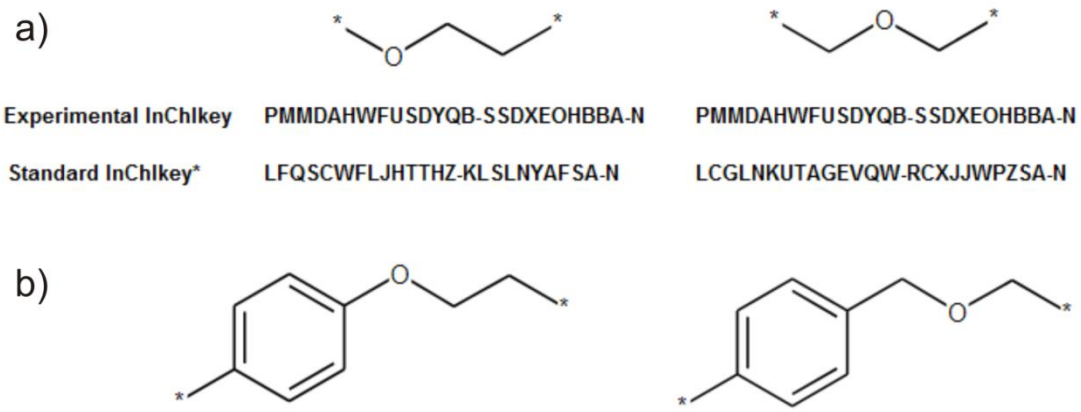


**Figure S5.** Two different representations of the polyethylene glycol repeat unit (**a**) and two different main chain repeat groups in combination with para-phenylene (**b**). The standard InChIkey is calculated by removing the atoms in the * position with the corresponding bonds and increasing the isotopic weight of the atom by 3 ($^{15}C$, $^{19}O$).

To distinguish between identical backbone fragments and to avoid storing multiple identical fragments in our database, we compute the standard InChIkey (not the experimental InChIkey) [63]. At the same time, for substituent attachment points, +1 was added to the mass of the atom to which the substituent is attached (i.e., the atom becomes some heavier isotope). In addition, instead of using the * symbol to indicate the main pathway; we add +3 to the isotopes of atoms that are at the beginning and end of the main chain. This procedure makes it possible to calculate the standard InChIkey of any fragment that does not contain nonphysical atoms (i.e. * marks the repeating chain, if they are present, the standard InChIkey is not calculated). It is also possible to distinguish between isomers of the main chain, e.g. ortho- and para-phenylenes. For example, for the polyethylene glycol repeating unit mentioned above, using the standard InChIkey to filter the resulting structures will store both oxyethylene representations in the fragment database (Figure S5), but will not store their duplicates.

*S4.2. Results of Predicting the Properties of Polymeric Materials Based on the Bitcerano and Askadskii Models*

To search for polymers suitable for use in different layers of protective coating, we generated all possible compounds consisting of one and two fragments of methylene and para-phenylene (Figure S4a and S4b). These fragments are chosen for two reasons. The first reason is simplicity. The second one is based on the analysis of Table S1. This table shows that the minimum permeability could be obtained for aliphatic polymers with the maximum number of chlorine atoms with positive contributions to the activation energy. Thus, according to the parameterization of the Askadskii model, polytetrachlorethylene should have a minimum water permeability. As additional substituent atoms, we choose fluorine and hydrogen atoms because they have the least negative contribution to the activation energy. They also have the smallest van der Waals volume to which the activation energy of Eq. (9) normalizes. Aromatic compounds are also considered because they

are more stable than aliphatic ones and allow a reduction in the number of F and H atoms that (according to Askadskii's ) make a negative contribution to the activation energy.

We generated 32580 polymers using the GENSTRUC program using the selected fragments shown in Figures S4a and S4b. Of the generated structures, only 1053 polymers were unique (see Section S4.1), the rest were filtered as duplicates. For the unique polymers, water vapor permeability was predicted using the Askadskii model, and oxygen permeability was predicted using the Bicerano model. Among them, 87 structures with water permeability less than < 350 Barrer were selected and collected in Table S2 (rows 3 – 89). Their oxygen permeability does not exceed 9 Barrer. It should be noted that traditional polymers such as polyperfluoroethylene (PTFE or Teflon, Figure S5e) and polyethylene (PE, Figure S5f) have predicted water permeability values of 328 and 60 Barrer and oxygen permeability values of 7.65 and 4.46 Barrer, respectively. As can be seen, they are not record holders for minimum water permeability. The high water permeability values obtained with the Askadskii model show that it is not entirely successful in the case of organofluorine compounds. However, in the absence of an alternative, it allows us to be optimistic about its use for other classes of polymers. Therefore, high water permeability values (< 350 Barrer) were used to include organofluorinated compounds in Table S2. Butyl cyanoacrylate (adhesive base) and polyethylene terephthalate (PET) are also included in Table 2 (rows 1–2). The open access polymer databases were then searched for each polymer to determine its availability, see the right column in Table S2.

According to our predictions, the record holder with the lowest water permeability is polytetrachlorethylene (Figure S6a). However, when searching for information on this compound, no mention of its synthesis was found. Of the other polymers used, polytrifluorochloroethylene has good performance (Figure S6c), but this material is not widely used in water repellent coatings. At the same time, polyvinylidene chloride (Figure S6b), which is commercially produced for water repellent coatings, degrades with the release of HCl [74]. As a result of the high toxicity of the degradation products of organochlorine compounds, their use in food packaging films is strongly discouraged.

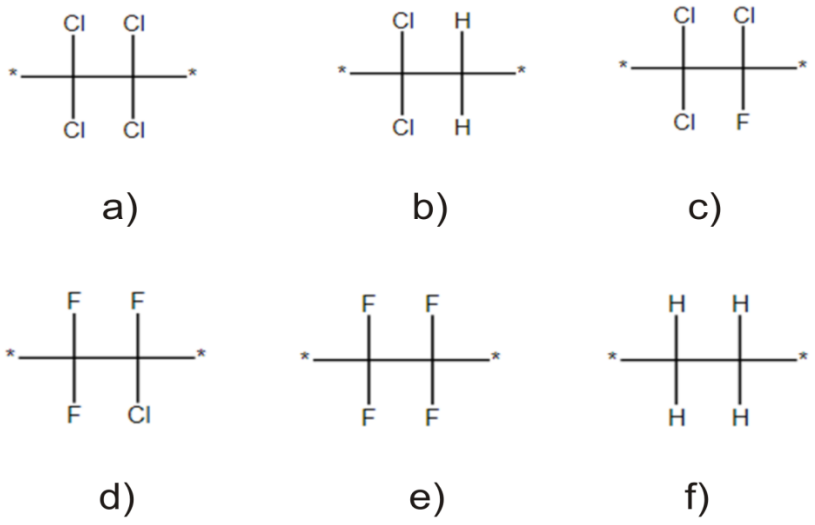


**Figure S6.** Structures of polymeric materials discussed in the publication: (**a**) polytetrachloroethylene, (**b**) polyvinylidene chloride, (**c**) polytrichlorofluoroethylene, (**d**) polychlorotrifluoroethylene, (**e**) polyperfluoroethylene, and (**f**) polyethylene.

Although Teflon has higher water and oxygen permeability, it is most commonly used because of its hydrophobic surface (i.e., liquid does not wet the surface while water vapor can pass through its pores), and good chemical, mechanical, and temperature resistance. Polyethylene terephthalate also has high water permeability and extremely low oxygen permeability. Due to its biological inertness, chemical resistance, transparency, and good mechanical properties, it is often used as the basis for packaging materials. Polyethylene is perhaps the cheapest synthetic polymer material and is actively used in noncritical products (e.g. food bags). To improve its performance, it can be used in multilayer coatings in combination with low water and oxygen permeability layers.

**Table S2.** Properties of virtually generated polymers.

| | **Polymer Structures** | ***P*($O_2$) (Barrer)** | ***P*($H_2O$) (Barrer)** | **Availability of polymers (received via Internet)** |
|---|---|---|---|---|
| Glue | | | | |
| 1 | 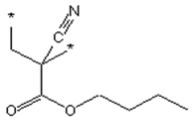 | 0.07 | 60.71 | Industrial Product<br>*Poly(butyl cyanoacrylate) (PBCA)* |
| Transparent, environmentally resistant structural material | | | | |
| 2 | 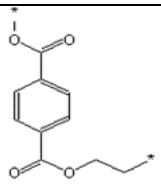 | 0.04 | 87.85 | Industrial Product<br>*Polyethylene terephthalate (PET)* |
| Selected polymers with low oxygen permeability | | | | |
| 3 | 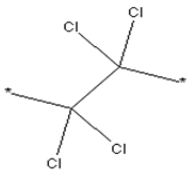 | 0.001 | 8.47 | No mentions found |
| 4 | 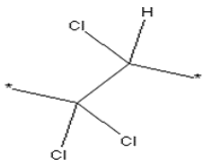 | 0.001 | 10.21 | No mentions found |

| | Polymer Structures | *P*($O_2$) (Barrer) | *P*($H_2O$) (Barrer) | Availability of polymers (received via Internet) |
|---|---|---|---|---|
| 5 | 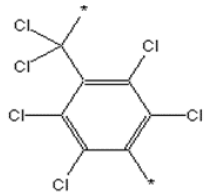 | 0.13 | 8.76 | No mentions found |
| 6 | 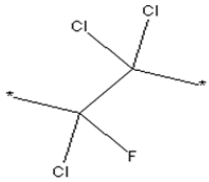 | 0.00 | 15.06 | No mentions found |
| 7 | 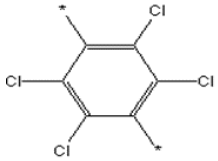 | 0.70 | 8.86 | No mentions found |
| 8 | 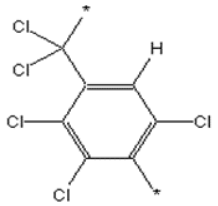 | 0.12 | 9.74 | No mentions found |
| 9 | 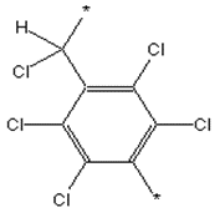 | 0.12 | 9.59 | No mentions found |
| 10 | 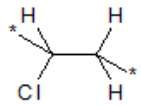 | 0.05 | 22.32 | Industrial Product<br>*Polyvinyl chloride (PVC)* |
| 11 | 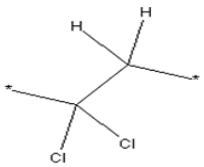 | 0.30 | 14.43 | Industrial Product<br>*Polyvinylidene chloride(PVDC)* |

| | Polymer Structures | *P*($O_2$) (Barrer) | *P*($H_2O$) (Barrer) | Availability of polymers (received via Internet) |
|---|---|---|---|---|
| 12 | 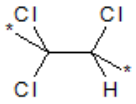 | 0.00118 | 10.21 | No mentions found |
| 13 | 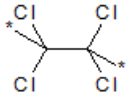 | 0.00047 | 8.47 | No mentions found |
| 14 | 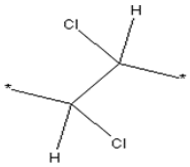 | 0.01 | 13.27 | Known polymer |
| 15 | 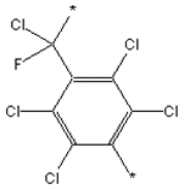 | 0.00 | 11.58 | No mentions found |
| 16 | 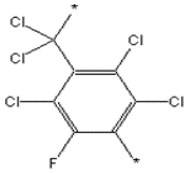 | 0.34 | 11.58 | No mentions found |
| 17 | 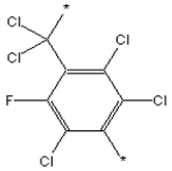 | 0.20 | 11.58 | No mentions found |
| 18 | 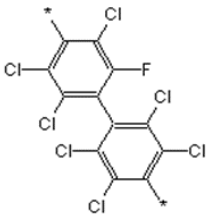 | 0.20 | 10.65 | No mentions found |

| | Polymer Structures | *P*($O_2$) (Barrer) | *P*($H_2O$) (Barrer) | Availability of polymers (received via Internet) |
|---|---|---|---|---|
| 19 | 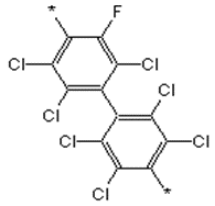 | 0.92 | 10.65 | No mentions found |
| 20 | 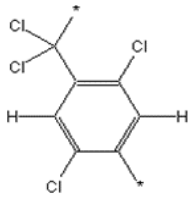 | 0.92 | 11.08 | No mentions found |
| 21 | 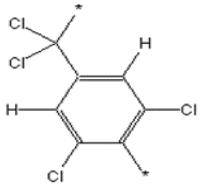 | 0.12 | 11.08 | No mentions found |
| 22 | 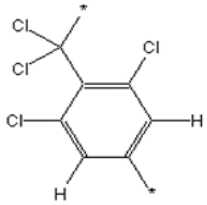 | 0.12 | 11.08 | No mentions found |
| 23 | 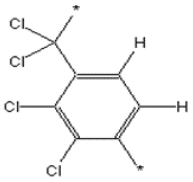 | 0.12 | 11.07 | No mentions found |
| 24 | 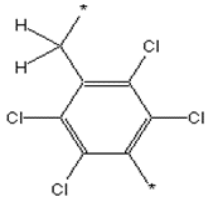 | 0.11 | 10.96 | No mentions found |
| 25 | 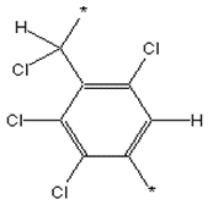 | 0.92 | 10.87 | No mentions found |

| | Polymer Structures | *P*($O_2$) (Barrer) | *P*($H_2O$) (Barrer) | Availability of polymers (received via Internet) |
|---|---|---|---|---|
| 26 | 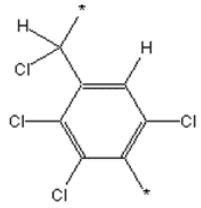 | 0.31 | 10.87 | No mentions found |
| 27 | 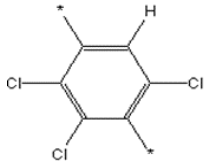 | 0.31 | 10.28 | No mentions found |
| 28 | 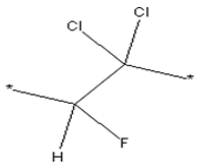 | 0.79 | 22.03 | No mentions found |
| 29 | 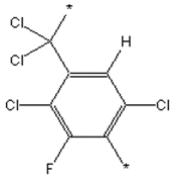 | 0.01 | 13.35 | No mentions found |
| 30 | 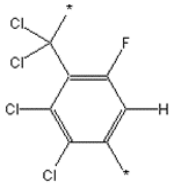 | 0.19 | 13.35 | No mentions found |
| 31 | 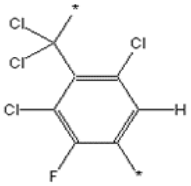 | 0.19 | 13.35 | No mentions found |
| 32 | 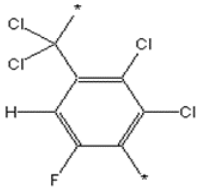 | 0.19 | 13.35 | No mentions found |

| | Polymer Structures | *P*($O_2$) (Barrer) | *P*($H_2O$) (Barrer) | Availability of polymers (received via Internet) |
|---|---|---|---|---|
| 33 | 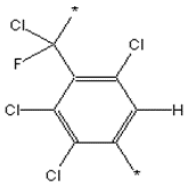 | 0.19 | 13.35 | No mentions found |
| 34 | 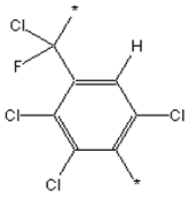 | 0.35 | 13.35 | No mentions found |
| 35 | 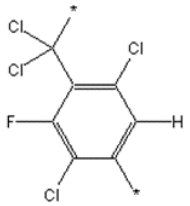 | 0.35 | 13.35 | No mentions found |
| 36 | 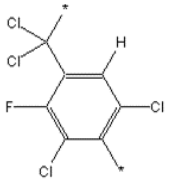 | 0.19 | 13.35 | No mentions found |
| 37 | 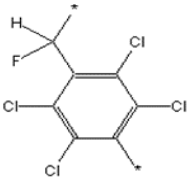 | 0.19 | 13.27 | No mentions found |
| 38 | 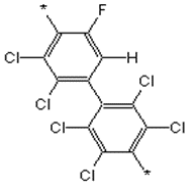 | 0.80 | 11.60 | No mentions found |

| | Polymer Structures | *P*($O_2$) (Barrer) | *P*($H_2O$) (Barrer) | Availability of polymers (received via Internet) |
|---|---|---|---|---|
| 39 | 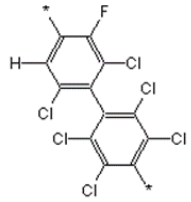 | 0.99 | 11.60 | No mentions found |
| 40 | 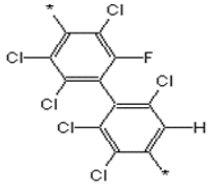 | 0.99 | 11.60 | No mentions found |
| 41 | 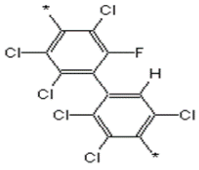 | 0.99 | 11.60 | No mentions found |
| 42 | 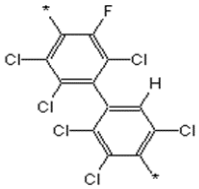 | 0.99 | 11.60 | No mentions found |
| 43 | 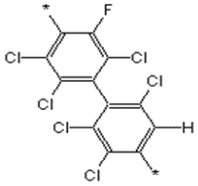 | 0.99 | 11.60 | No mentions found |
| 44 | 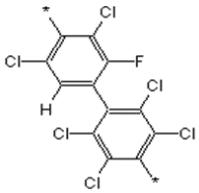 | 0.99 | 11.60 | No mentions found |
| 45 | 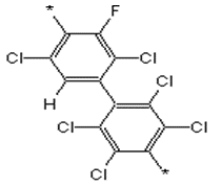 | 0.99 | 11.60 | No mentions found |

| | Polymer Structures | $P(O_2)$ (Barrer) | $P(H_2O)$ (Barrer) | Availability of polymers (received via Internet) |
|---|---|---|---|---|
| 46 | 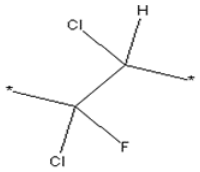 | 0.99 | 21.03 | No mentions found |
| 47 | 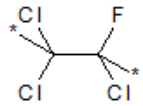 | 0.00347 | 15.06 | No mentions found |
| 48 | 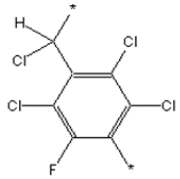 | 0.01 | 13.07 | No mentions found |
| 49 | 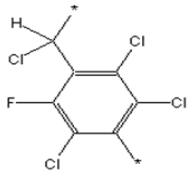 | 0.48 | 13.07 | No mentions found |
| 50 | 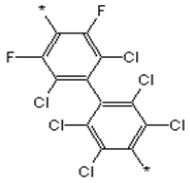 | 0.48 | 13.00 | No mentions found |
| 51 | 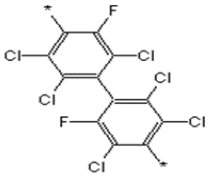 | 1.23 | 13.00 | No mentions found |
| 52 | 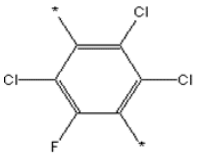 | 1.23 | 13.00 | No mentions found |

| | Polymer Structures | $P(O_2)$ (Barrer) | $P(H_2O)$ (Barrer) | Availability of polymers (received via Internet) |
|---|---|---|---|---|
| 53 | 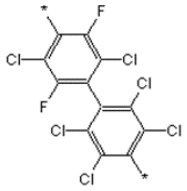 | 1.23 | 13.00 | No mentions found |
| 54 | 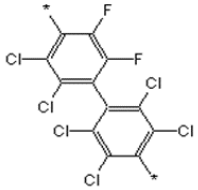 | 1.23 | 13.00 | No mentions found |
| 55 | 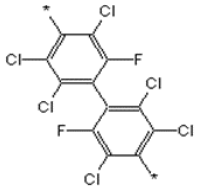 | 1.23 | 13.00 | No mentions found |
| 56 | 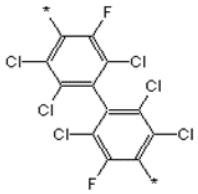 | 1.23 | 13.00 | No mentions found |
| 57 | 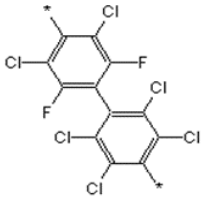 | 1.23 | 13.00 | No mentions found |
| 58 | 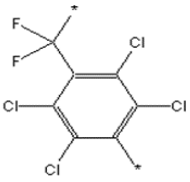 | 1.23 | 15.85 | No mentions found |
| 59 | 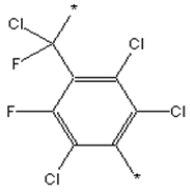 | 0.90 | 15.85 | No mentions found |

| | Polymer Structures | *P*($O_2$) (Barrer) | *P*($H_2O$) (Barrer) | Availability of polymers (received via Internet) |
|---|---|---|---|---|
| 60 | 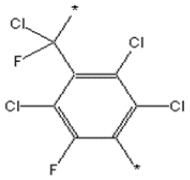 | 0.53 | 15.85 | No mentions found |
| 61 | 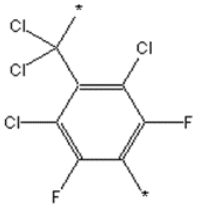 | 0.53 | 15.85 | No mentions found |
| 62 | 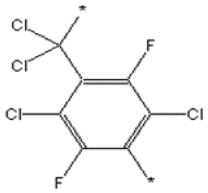 | 0.31 | 15.85 | No mentions found |
| 63 | 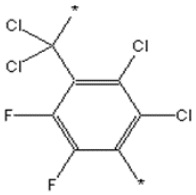 | 0.31 | 15.85 | No mentions found |
| 64 | 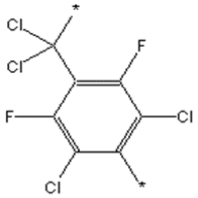 | 0.31 | 15.85 | No mentions found |
| 65 | 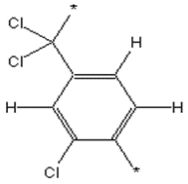 | 0.31 | 12.99 | No mentions found |
| 66 | 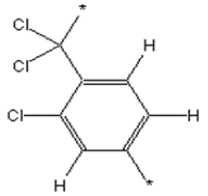 | 0.06 | 12.99 | No mentions found |

| | Polymer Structures | $P(O_2)$ (Barrer) | $P(H_2O)$ (Barrer) | Availability of polymers (received via Internet) |
|---|---|---|---|---|
| 67 | 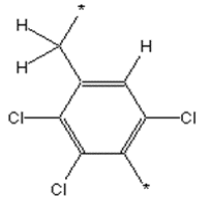 | 0.06 | 12.99 | No mentions found |
| 68 | 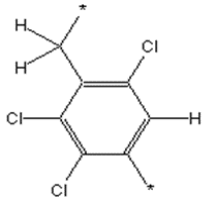 | 1.05 | 12.84 | No mentions found |
| 69 | 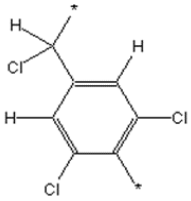 | 1.05 | 12.71 | No mentions found |
| 70 | 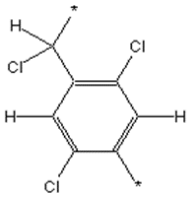 | 0.32 | 12.71 | No mentions found |
| 71 | 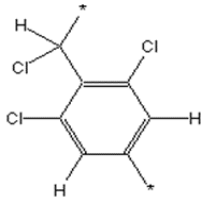 | 0.32 | 12.71 | No mentions found |
| 72 | 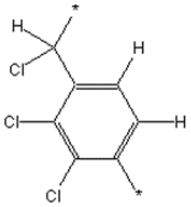 | 0.32 | 12.69 | No mentions found |

| | Polymer Structures | *P*($O_2$) (Barrer) | *P*($H_2O$) (Barrer) | Availability of polymers (received via Internet) |
|---|---|---|---|---|
| 73 | 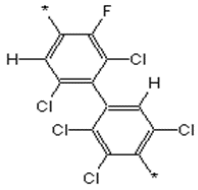 | 0.31 | 12.78 | No mentions found |
| 74 | 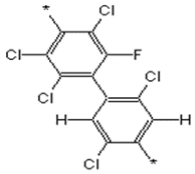 | 1.09 | 12.78 | No mentions found |
| 75 | 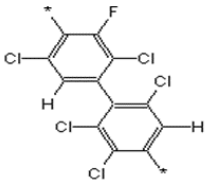 | 1.09 | 12.78 | No mentions found |
| 76 | 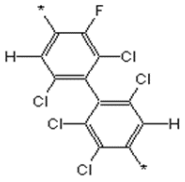 | 1.09 | 12.78 | No mentions found |
| 77 | 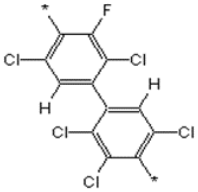 | 1.09 | 12.78 | No mentions found |
| 78 | 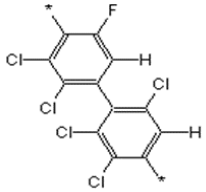 | 1.09 | 12.78 | No mentions found |
| 79 | 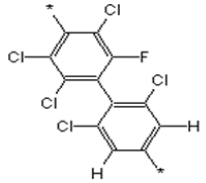 | 1.09 | 12.78 | No mentions found |

| | Polymer Structures | *P*($O_2$) (Barrer) | *P*($H_2O$) (Barrer) | Availability of polymers (received via Internet) |
|---|---|---|---|---|
| 80 | 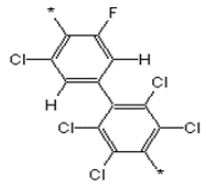 | 1.09 | 12.78 | No mentions found |
| 81 | 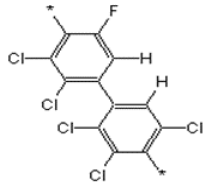 | 1.09 | 12.78 | No mentions found |
| 82 | 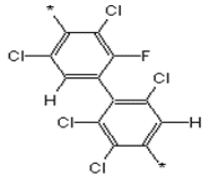 | 1.09 | 12.78 | No mentions found |
| 83 | 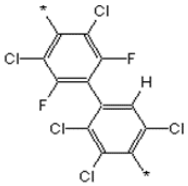 | 1.09 | 14.40 | No mentions found |
| 84 | 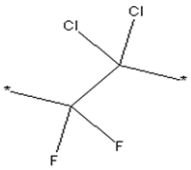 | 0.03 | 31.49 | No mentions found |
| 85 | 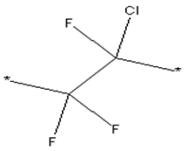 | 0.39 | 83.90 | Industrial Product<br>*Poly(trifluorochloroethylene) (PCTFE)* |
| 86 | 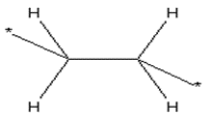 | 4.47 | 60.12 | Industrial Product<br>*Polyethylene* |
| 87 | 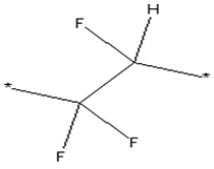 | 5.67 | 260.07 | Known polymer<br>*Polytrifluoroethylene* |

| | Polymer Structures | $P(O_2)$ (Barrer) | $P(H_2O)$ (Barrer) | Availability of polymers (received via Internet) |
|---|---|---|---|---|
| 88 | 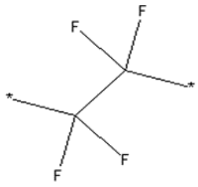 | 7.65 | 328.64 | Industrial Product<br>*Poly(tetrafluoroethylene)* |
| 89 | 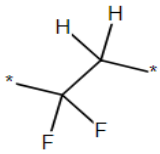 | 8.91 | 192.64 | Industrial Product<br>*Polyvinylidene fluoride* |

**S5. Influence of the Choice of the Valence Force Field on the Results of Atomistic Calculations**

We performed a series of comparative calculations in the case of the solubility parameters to determine how the choice of valence force field (VFF) affects our results. For comparison, the Class II polymer consistent force field (PCFF) [75], condensed-phase optimized molecular potentials for atomistic simulation studies (COMPASS) [79], and DREIDING [80] were used. The general functional form of all these VFFs is similar and takes into account the bonded interactions $E_{Bond}$, such as tension $E_{Angle}$, bending and torsion $E_{Torsion}$, as well as non-bonded interactions including van der Waals $E_{vdw(L-J)}$ and Coulomb interactions $E_{Coulomb}$:

$$E_{Total} = E_{Bond} + E_{Angle} + E_{Torsion} + E_{vdw(L-J)} + E_{Coulomb}. \quad (S10)$$

However, each term contains unique force field parameters and has different ways of describing uncoupled and torsional interactions, mixing rules, and separate scaling factors.

The dependencies of the number of equilibrium oxygen and water molecules in the simulation cell $N_{ell}(p)$ obtained with COMPASS and DREIDING VFFs are shown in Figure S7. As with the PCFF, the agreement with the experimental data for two additional VFFs is in the order of magnitude (see Table S3 and Table S4). Both the DREIDING and COMPASS force fields show qualitatively incorrect solubility trends for oxygen for selected materials.

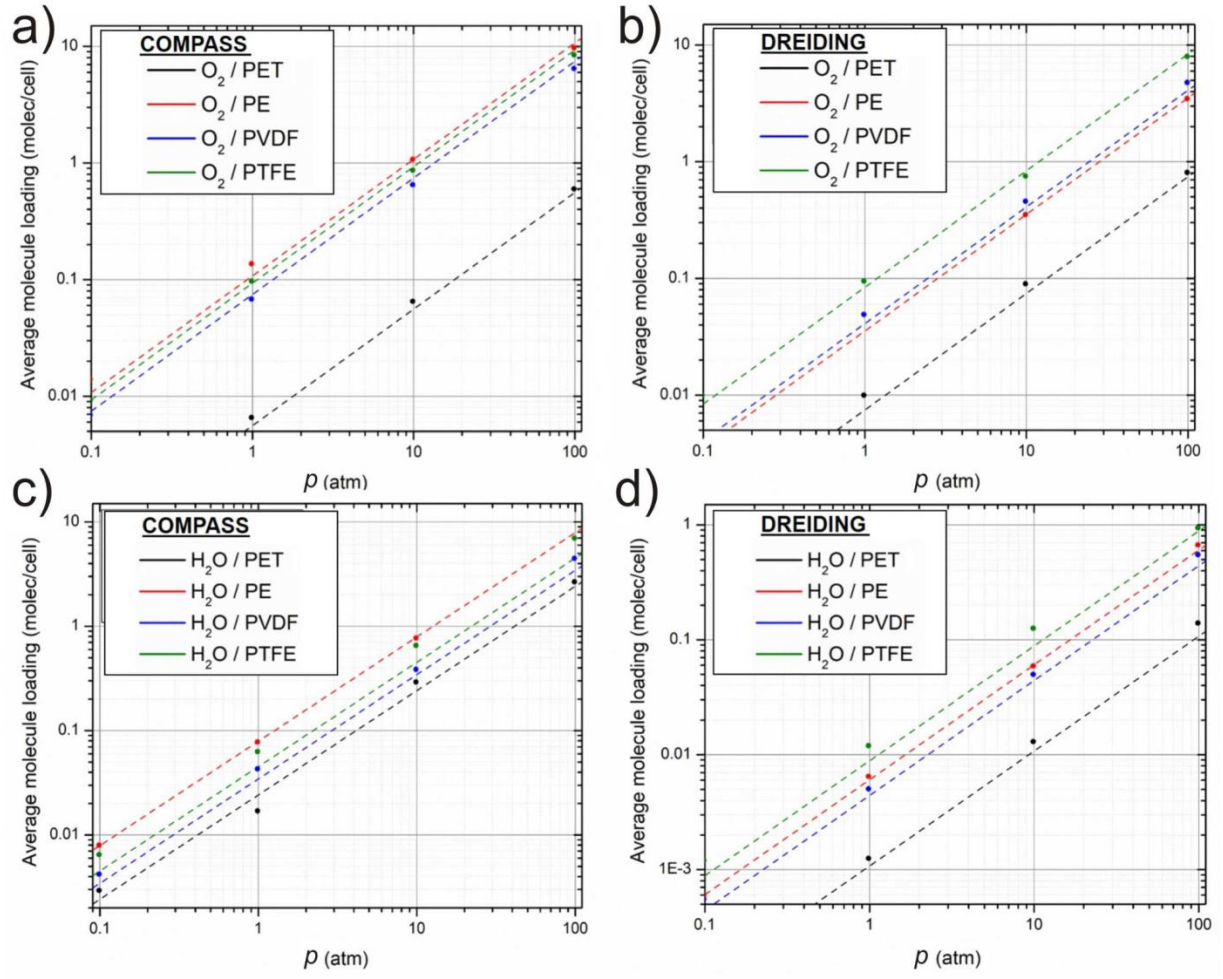


**Figure S7.** Calculated dependencies of the number of equilibrium oxygen (**a**,**b**) and water (**c**,**d**) molecules on the pressure *p* in the simulation cell for PET, PE, PVDF, and PTFE materials obtained using COMPASS (**a**,**c**) and DREIDING (**b**,**d**) force fields.

Absolute values of the *S* solubility coefficient for oxygen and water molecules calculated with the COMPASS VFF are overestimated by almost an order of magnitude. It can be concluded that this VFF may be less accurate than the other two VFFs for estimating the barrier properties for PET, PE, PVDF, and PTFE. It is also interesting to note that the tested VFFs show different trends of the water vapor solubility coefficients in the selected materials. This can be explained by the different parameters of the O-O and O-H interactions inherent in these interaction potentials, as well as possible differences in the typing of the atoms, but this issue requires more detailed consideration for further improvement of the technique.

Thus, the prediction of water vapor solubility in polymers is more difficult to describe with atomistic methods. In terms of quantitative agreement, for all potentials considered, we can only speak of an order of magnitude agreement, and both overestimation and underestimation of the calculated values are possible. This confirms that an accurate prediction of barrier properties requires correct characterisation of the interaction between the penetrant molecule and the barrier material.

**Table S3.** Calculated solubility coefficients S ($cm^3(STP)/(cm^3 \cdot Pa)$) for oxygen molecules in polyethylene terephthalate (PET), polyethylene (PE), polyvinylidene fluoride (PVDF) and polytetrafluoroethylene (PTFE).

| | **Force Field** | | | |
|---|---|---|---|---|
| **Material** | PCFF | COMPASS | DREIDING | Experiment [82] |
| PET | $2.2 \pm 0.8 \cdot 10^{-8}$ | $1.2 \pm 0.2 \cdot 10^{-7}$ | $1.6 \pm 0.3 \cdot 10^{-7}$ | $6–10 \cdot 10^{-7}$ |
| PE | $2.0 \pm 1.0 \cdot 10^{-8}$ | $2.3 \pm 0.4 \cdot 10^{-6}$ | $7.6 \pm 0.2 \cdot 10^{-7}$ | $2–5 \cdot 10^{-7}$ |
| PVDF | $2.5 \pm 1.5 \cdot 10^{-8}$ | $1.6 \pm 0.9 \cdot 10^{-6}$ | $8.8 \pm 1.5 \cdot 10^{-7}$ | $3.6 \cdot 10^{-7}$ |
| PTFE | $6.0 \pm 1.0 \cdot 10^{-7}$ | $2.0 \pm 0.4 \cdot 10^{-6}$ | $1.8 \pm 0.2 \cdot 10^{-6}$ | $6–9 \cdot 10^{-7}$ |

**Table S4.** Calculated solubility coefficients S ($cm^3(STP)/(cm^3 \cdot Pa)$) for water vapor in polyethylene terephthalate (PET), polyethylene (PE), polyvinylidene fluoride (PVDF) and polytetrafluoroethylene (PTFE).

| | **Force Field** | | | |
|---|---|---|---|---|
| **Material** | PCFF | COMPASS II | DREIDING | Experiment [82] |
| PET | $7.2 \pm 0.7 \cdot 10^{-6}$ | $5.2 \pm 0.8 \cdot 10^{-7}$ | $2.3 \pm 0.4 \cdot 10^{-8}$ | $3–8 \cdot 10^{-9}$ |
| PE | $1.5 \pm 2 \cdot 10^{-6}$ | $1.7 \pm 0.3 \cdot 10^{-6}$ | $1.3 \pm 0.3 \cdot 10^{-7}$ | $5.8 \cdot 10^{-8}$ |
| PVDF | $6.5 \pm 0.6 \cdot 10^{-6}$ | $7.4 \pm 1.3 \cdot 10^{-7}$ | $9.5 \pm 1.5 \cdot 10^{-8}$ | – |
| PTFE | $8 \pm 1.5 \cdot 10^{-6}$ | $9.7 \pm 1.7 \cdot 10^{-7}$ | $1.9 \pm 0.3 \cdot 10^{-7}$ | – |